mater.scichina.com link.springer.com

Sci China Mater 2025, 68(9): 3212–3218 https://doi.org/10.1007/s40843-025-3429-x



SPECIAL ISSUE: Celebrating the 130th Anniversary of Tianjin University

Photopatternable gel electrolytes for stretchable solid-state organic electrochemical transistors

Liqun Tang¹, Xue Zheng¹, Mingyuan Sun¹, Xiaochen Ren^{1,2,3}, Wei Huang⁴, Long Ye^{1,5}, Chuanfei Guo⁶, Yi-Xuan Wang^{1,2,3*} and Wenping Hu^{1,2,3*}

ABSTRACT Organic electrochemical transistors (OECTs), functioning as transduction amplifiers, demonstrate considerable potential for integration into biosensors and wearable technologies. However, conventional OECTs demonstrate limited stability in conformal sensing on biointerfaces, primarily due to their poor ductility and liquid-electrolyte-gated operation mechanisms. A double-network-based stretchable gel electrolyte is presented, simultaneously integrating exceptional mechanical compliance and high ionic conductivity. OECT arrays, gated through photopatterned gel electrolytes, demonstrate high uniformity in electrical performance. Besides, the solid-state devices show remarkable electrical stability when subjected to 50% strain, thus facilitating continuous electrocardiogram monitoring under mechanical deformation. This validates its application potential in ambulatory healthcare systems requiring long-term biosensing.

Keywords: stretchable electronics, gel electrolytes, organic electrochemical transistors, electrocardiogram recording

INTRODUCTION

Bioelectronic devices function as critical sensing components for electrophysiological monitoring in clinical and ambulatory healthcare settings [1–3]. Wearable devices with conformal and stable biointerfaces effectively reduce motion artifacts through mechanical stress distribution. This capability supports prolonged biosensing with enhanced signal-to-noise ratios (SNR) [4–7]. Organic electrochemical transistors (OECTs) represent a breakthrough in wearable biosensing, capitalizing on high transconductance, low-voltage operation, and biocompatible interfaces [8]. These attributes facilitate precise electrophysiological monitoring on deformable biological substrates [9,10]. OECT modulates the source-drain current ($I_{\rm D}$) by electrochemically doping/dedoping its semiconductor channel, where the gate voltage ($V_{\rm G}$)-controlled ion injection from the electrolytes dynamically alters carrier density and conductivity

of conducting polymers. Both electrolyte composition and channel material properties directly govern three critical parameters in OECT biosensors: transconductance, SNR, and operational stability [11,12].

Wearable electronic devices must conform to skin surfaces while enduring mechanical deformations such as bending, twisting, and stretching with strains reaching approximately 30% [13-15]. Therefore, the development of soft and stretchable architectures of OECTs with stable electrochemical coupling becomes crucial for applications in biosensing technologies and bioelectronic systems [16-18]. In comparison with liquid electrolyte-gated OECTs, solid-state OECTs based on gel electrolyte demonstrate superior environmental stability, including resistance to thermal degradation and humidity-induced performance variation [19-21]. Importantly, Young's modulus of gel electrolyte spans from 1 Pa to 300 MPa, encompassing characteristic values of biological tissues including skin and muscle (200-500 kPa), as well as neural tissues such as brain parenchyma and spinal cord (500 Pa-200 kPa) [22,23] . Therefore, numerous studies have focused on the design of gel-based ionic conductors as an electrolyte layer for solid-state OECTs [24-27]. Examples of synthesized gel electrolytes include gelatin, chitosan (CS), agar, poly(ethylene glycol) (PEG), polyacrylamide (PAAm), and poly(hydroxyethyl methacrylate) (PHEMA). These gel electrolytes offer excellent controllability, mechanical properties, environmental stability and biocompatibility for reducing interface resistance and enhancing compliance with biological systems [28-32]. However, conventional fabrication of gel electrolyte employs solution-based techniques like inkjet and screen printing, exhibiting limited resolution for integrated high-density soft/stretchable device arrays [33-35].

In this study, we present the fabrication of stretchable solidstate OECTs utilizing a photopatternable gel electrolyte, consisting of CS and polyhydroxyethyl acrylate (CS-PHEA). The photo-crosslinkable structure design enables precise patterning and *in situ* manufacturing capabilities for devices with complex architectures. The engineered gel electrolyte also demonstrates

¹ Key Laboratory of Organic Integrated Circuits, Ministry of Education & Tianjin Key Laboratory of Molecular Optoelectronic Sciences, Department of Chemistry, School of Science, Tianjin University, Tianjin 300072, China

² Collaborative Innovation Center of Chemical Science and Engineering (Tianjin), Tianjin 300072, China

³ Haihe Laboratory of Sustainable Chemical Transformations, Tianjin 300192, China

⁴ School of Automation Engineering, University of Electronic Science and Technology of China (UESTC), Chengdu 611731, China

⁵ School of Materials Science and Engineering, Tianjin University, Tianjin 300350, China

⁶ Department of Materials Science and Engineering, Southern University of Science and Technology, Shenzhen 518055, China

^{*} Corresponding author (email: yx_wang@tju.edu.cn; huwp@tju.edu.cn)

SCIENCE CHINA Materials

ARTICLES

remarkable mechanical compliance, featuring 640% fracture strain and skin-matched Young's modulus (114 kPa). When integrated with polyrotaxane (PR)-plasticized conducting polymers (poly(3,4-ethylenedioxythiophene):poly(styrenesulfonate) (PEDOT:PSS)), the resulting solid-state OECT achieved a high $[\mu C^*]$ value of 317.71 \pm 11.61 F cm $^{-1}$ V $^{-1}$ s $^{-1}$, with consistent transconductance (~6.5 mS) under 50% strain. They also demonstrate exceptional cyclic stability during 60 min of continuous operation under stress, and exhibit high SNR (~30 dB) during analog electrocardiogram (ECG) monitoring, establishing an effective dynamic sensing platform for bioelectronic interfaces.

EXPERIMENTAL SECTION

Material

The synthesis of PR was conducted according to previously reported literature [36,37]. Chitosan (low molecular weight), 2-hydroxyethyl acrylate (HEA), glycerol, sodium chloride (NaCl), acetic acid and 2,6-bis(4-azidobenzylidene)cyclohexanone (wetted with approximately 30% water, containing 25 g on a dry weight basis) were purchased from HEOWNS. PEDOT:PSS (Clevios PH1000) was purchased from Heraeus. Sulfuric acid, photoinitiator 1173 were purchased from Sigma-Aldrich. Capstone TM FS-30 was purchased from Chemours. Polystyrene-block-poly(ethylene-ran-butylene)-block-polystyrene (SEBS, H1062) was purchased from Aladdin. AZ5214, along with their developers (AZ 300MIF), were provided by Shanxi Sidi Information Co., Ltd.

Gel electrolyte preparation

Chitosan (1 wt%) solution was prepared by dissolving chitosan powder ($M_{\rm W}$ 50–190 kDa, \geq 75% deacetylation) in deionized water containing 6 wt% acetic acid under continuous magnetic stirring for 6 h until complete dissolution. Chitosan ion membrane was heated at 70 °C by drop casting. For the chitosanglycerol ionic membrane, chitosan aqueous solution was mixed with glycerol (6 wt%) and homogenized by magnetic stirring to obtain the chitosan-glycerol aqueous solution, and then the film was heated after drop casting. The preparation of gel electrolyte is as follows: chitosan aqueous solution was mixed with HEA and photoinitiator 1173 (the content was 1 wt% of HEA content) at a certain mass ratio, and the mixture was subjected to ultrasonic treatment for 10 min to obtain a mixed uniform solution. The solution was deposited onto target substrates via spincoating or drop-casting, followed by exposure at 365 nm LED source (110 mW cm⁻²) for 120 s to form crosslinked gel. The gel was subsequently immersed in an aqueous solution containing 6 wt% glycerol and 0.1 M NaCl for 1 h at 25 °C to construct a CS-PHEA double-network gel electrolyte.

Device fabrication

The pre-cleaned glass substrate was covered with a metal shadow mask, and 5 nm of Cr and 50 nm of Au were thermally evaporated as source-drain and side gate electrodes. To prepare the semiconductor channel, PEDOT:PSS solution mixed with PR (5 wt%) and CapstoneTM FS-30 (0.5 wt%) was spin-casted onto ultraviolet ozone (UVO)-treated substrates, followed by UV exposure for 5 min and annealing at 130 °C on a hot plate for 10 min. The conducting polymer was then treated with concentrated sulfuric acid (>95%, Duksan Pure Chemicals). A

positive photoresist (AZ5214) was used to define the channel pattern. The gel electrolytes were formed by spin-casting the configured solution, followed by photopatterning with a shadow mask. For stretchable OECTs, SEBS substrates were prepared by drop-casting of the 3 wt% azide/SEBS (200 mg mL⁻¹) solution, with photo-crosslinking by exposure to 284 nm UV light. The substrate was pre-stretched and the stress was released after the deposition of electrodes and semiconductor channel. The photopatterned gel electrolytes were then constructed to yield stretchable devices.

Characterizations and measurement

The electrical characterization of OECT was performed using a semiconductor analyzer (Keysight 4200A-SCS). The drain and gate electrodes were connected to the SMU module of the semiconductor analyzer, which can simultaneously apply voltage signals and measure the current signal at the same time. The source electrodes were connected to the ground. During transfer curves, the drain voltage $V_{\rm D}$ was set to $-0.5\,\mathrm{V}$ and the gate voltage V_G was swept from 1 to -1 V with voltage steps of 0.01 V at a sweep rate of 20 mV s⁻¹. During output curves, V_D was swept from 0 to -0.6 V in increments of 0.01 V at a sweep rate of 50 mV s⁻¹. This process was repeated for V_G spanning from 0.2 to -0.6 V with increments of 0.2 V. For measuring stretchable OECT under strain, devices were maintained under a strain by using a small tensile stage. The applied strain percentage is defined as the length change ΔL upon strain with respect to the original length L of the unstretched films: $(\Delta L/L) \times 100\%$. The film thicknesses were measured by using a profilometer (Bruker, Dektak X). The UV-vis absorption spectra were measured with a SHZMADZU UV-3600 Plus spectrophotometer. The transmittance was measured in a dual-beam mode to correct the variance in the lamp flux, and a blank quartz plate was used as a 100% transmittance reference sample. Optical microscopy images were captured using a LEICA DM2700M. The electrochemical properties of the samples were measured using an electrochemical workstation (CHI660E, CH Instruments, Inc.). In electrochemical impedance spectroscopy (EIS) tests, the impedance frequency range was 10 kHz to 0.1 Hz. Mechanical properties were studied by an MTS Criterion Model 42, with a strain rate of 0.05 mm s⁻¹.

ECG measurements

A lead-II ECG signal channel was generated using the SKX-2000C+ simulator, with an amplitude of 2 mV and a frequency of 60 bpm. The simulator, along with a bias voltage ($V_{\rm bias}$), was connected in series between the gate and the source of the OECT. The ECG signal was acquired from the $I_{\rm D}$ of the OECT. The SNR was calculated as the ratio of the peak-to-peak current amplitude of the ECG signal to that of the noise region.

RESULTS AND DISCUSSION

As a natural cationic polyelectrolyte, chitosan exhibits exceptional biocompatibility, chemical stability, and solution processability, rendering it extensively utilized in biomedical engineering, environmental remediation, and food technology applications [38]. Chitosan-based ion-conductive membranes have emerged as promising candidates for solid-state electrolytes in OECTs, particularly in bioelectronic applications [39]. However, the inherent mechanical limitations of pure chitosan ionic membranes with low water content exhibiting low fracture

elongation (~11%) and elevated Young's modulus (33 MPa) as quantified in Fig. S1, significantly constrain their applicability in flexible stretchable device fabrication. Therefore, we developed a low-modulus gel electrolyte through a physically cross-linked double-network strategy (Fig. 1a, Fig. S2). This structural configuration comprises a linear polymer framework (PHEA) interpenetrated with chitosan polymers. The hydroxyl-rich structure of PHEA establishes multivalent hydrogen bonds with chitosan, achieving collaborative optimization of mechanical performance (Fig. S3) and ionic conductivity [40,41]. We systematically investigated the impact of PHEA content on mechanical performance, revealing an inverse correlation between PHEA concentration and ductility. As shown in Fig. 1b, c, when the mass ratio of CS to PHEA was reduced from 1:10 to 1:40, the elongation at break dropped from 640% to 292%, accompanied by a 2.06 folds enhancement in Young's modulus (from 114 to 235 kPa). These trends demonstrate that excessive PHEA incorporation induces denser polymer networks, resulting in mechanically toughened electrolytes with compromised deformability. As shown in Fig. 1d, the ionic conductivity of the gel decreased from 2.58×10⁻⁴ to 7.7×10⁻⁵ S cm⁻¹ with increasing PHEA content, a phenomenon due to the introduction of more insulating PHEA domains. The optimal CS:PHEA ratio was identified as 1:10 (w/w), balancing mechanical compliance $(\varepsilon=640\%)$ and ionic conductivity $(2.58\times10^{-4} \text{ S cm}^{-1})$. As shown in Fig. 1e, the epidermal impedance of the gel electrolyte-skin interface was determined as ~5 kΩ at 1 kHz. Such a low impedance is conducive to noise suppression and improvement of the SNR in the application of wearable devices [42,43]. As shown in Fig. 1f, CS-PHEA gel electrolytes exhibited patterns with feature sizes of less than 1 mm through a rapid photopolymerization process. In the hydrated state, the thickness of the gel electrolyte is approximately 300-400 µm. The developed photo-patterning technique enables rapid and straightforward fabrication of gel electrolytes, offering precise *in situ* manufacturing capabilities for devices with complex architectures and specialized configurations. This advancement facilitates seamless integration of components while maintaining structural integrity, thereby supporting high-density integration and scalable production processes. The CS-PHEA gel electrolyte achieves ~95% transmittance across 400–800 nm (Fig. 1g), making it suitable for transparent epidermal electronics and optoelectronic sensors [44,45].

The schematic diagram of solid-state OECT based on CS-PHEA gel electrolyte is shown in Fig. 2a. Gate voltage modulates ion migration dynamics in the electrolyte, facilitating electrochemical doping via reversible ion intercalation/deintercalation in the semiconductor channel. The conducting polymer PEDOT: PSS is extensively employed in OECTs due to its high intrinsic conductivity and solution processability. We used a polymer plasticizer, i.e., PR, to improve the ductility of PEDOT:PSS (Fig. S4), with subsequent sulfuric acid treatment for enhanced electrical conductivity [36]. As demonstrated in Fig. 2b, the solidstate OECT achieves a high transconductance of 13.2 mS. Fig. 2c shows the output characteristics of CS-PHEA gel electrolyte gated solid-state OECT. These devices exhibit typical pinch-off behavior while the drain current (I_D) decreases with an increased gate voltage (V_G) from -0.2 to 0.8 V, which is attributed to dedoping in the PEDOT:PSS channel. To quantitatively evaluate the device performance, we systematically collected their saturation regime transfer curves with varying channel dimensions (Fig. 2d). The product of charge carrier mobility and volumetric charge storage capacity ($[\mu C^*]$) was adopted as the figure of merit for device characterization. The solid-state OECT demonstrates a high $[\mu C^*]$ value of 317.71±11.61 F cm⁻¹ V⁻¹ s⁻¹. Benefiting from the photo-patentability of gel electrolyte with

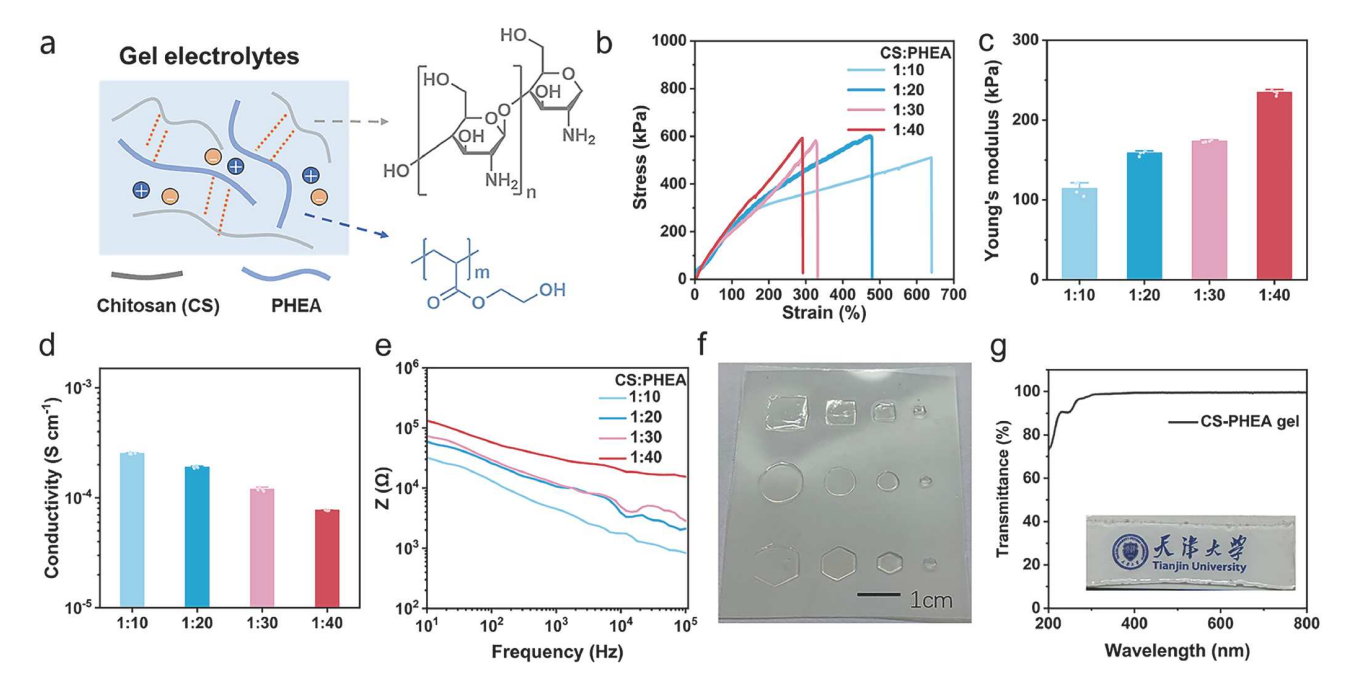


Figure 1 Synthesis and characterization of CS-PHEA gel electrolytes. (a) Schematic illustration of a physically cross-linked double-network CS-PHEA gel electrolyte structure. (b) Tensile stress-strain curves for CS-PHEA with different compositions (10–40 wt% PHEA). (c) Young's modulus analysis of composition-optimized CS-PHEA gel electrolytes. (d) Ionic conductivity of gel electrolytes with varied PHEA contents. (e) Impedance of gel electrolytes-skin interface. (f) Image of photopatterned CS-PHEA gel electrolytes. (g) Transmittance of the CS-PHEA gel electrolyte. Inset: photograph of a gel electrolyte film.

ARTICLES

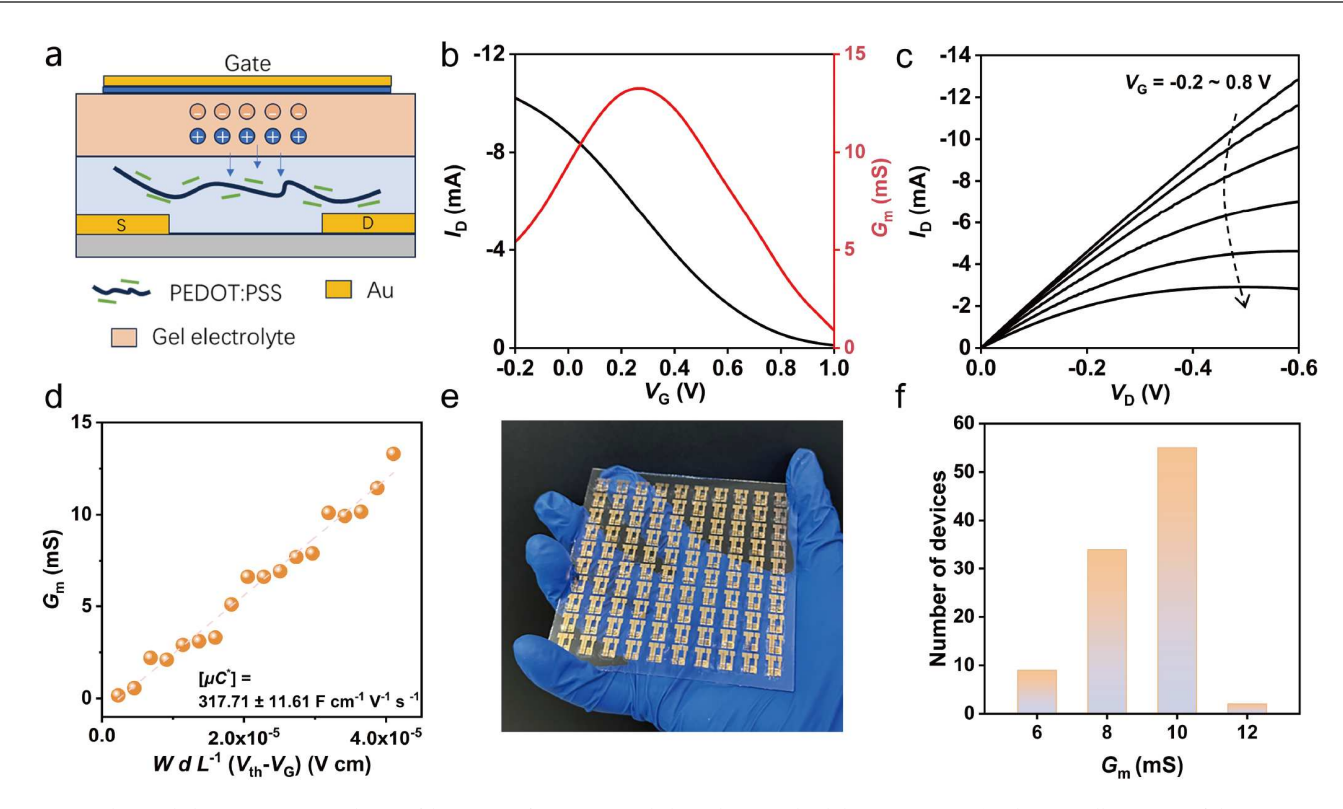


Figure 2 Electrical characterization and array fabrication of CS-PHEA gel electrolyte gated solid-state OECT. (a) Schematic illustration of the CS-PHEA gel electrolyte gated OECT architecture. (b) Transfer and transconductance characteristics of the OECT (channel length (L)=50 μ m, width (W)=1800 μ m). (c) Output characteristic curves demonstrating current-voltage relationships. (d) Transconductance as a function of channel dimensions and operating parameters for CS-PHEA gel electrolyte gated OECT in the saturation region, used to extract the associated $[\mu C^*]$. (e) Photographic image of the fabricated CS-PHEA gel electrolyte gated solid-state OECT array. (f) Statistical distribution of transconductance values across the OECT array.

precise *in-situ* preparation, a solid-state OECT array (10×10 configuration) employing a side gate architecture was easily prepared [30]. Note that a PEDOT:PSS layer was deposited between the Au side-gate electrodes and CS-PHEA gel electrolyte to minimize interfacial electrochemical impedance [46,47]. The average transconductance ($G_{\rm m}$) of the 100 channels of the OECT array is 7.89 mS (L=100 μ m, W=1800 μ m). The narrow $G_{\rm m}$ distribution indicates the high uniformity in electrical performance, thus demonstrating the great potential of CS-PHEA electrolyte in the fabrication of large-scale solid-state OECT circuits.

Robust mechanical compliance integrated with stable charge transport dynamics is critical for maintaining signal fidelity in next-generation wearable bioelectronics operating under dynamic deformation [48,49]. Therefore, stretchable solid-state OECTs were fabricated with cross-linked SEBS as elastic substrates. As illustrated in Fig. 3a, the soft devices demonstrate a seamless contact with skin, indicating a high level of tolerance to mechanical deformation. To ensure stable signal recording during stretching, stretchable devices employ a pre-stretching strategy [50]. Metal electrodes are deposited on elastomer substrate, with a pre-stretching range of 50% (Fig. 3b), and the entire device is released after depositing the semiconductor film [51]. The stretchable gel electrolytes can be prepared by in-situ photopolymerization. The resulting devices exhibit stable transconductance outputs at about 6.5 mS (Fig. 3c, d). The operational stability of the solid-state OECT was evaluated through cyclic gate voltage (V_G) switching between 0 and 0.8 V at a constant drain voltage ($V_{\rm D} = -0.5 \, {\rm V}$). The results show negligible current degradation after 3600 ON/OFF cycles over 60 min (Fig. 3e), demonstrating the reliable and efficient ion conduction of CS-PHEA electrolyte under strain.

The CS-PHEA gel electrolyte-gated solid-state OECT was engineered for ECG signal acquisition. An ECG simulator was employed to generate signals, ensuring consistent signal quality unaffected by acquisition conditions, skin characteristics, or body movement [52]. As shown in Fig. 4a, the simulator along with a bias voltage ($V_{\rm bias}$) was connected in series and between the gate and the source of the OECT. $V_{\rm D}$ was set at $-0.5~{\rm V}$ to operate the solid-state OECT, and the ECG signal was recorded as the I_D . As a control electrolyte, an ion-conducting membrane consisting of chitosan with the glycerol plasticizer was used, as reported in the literature [29]. As demonstrated in Fig. S5, the CS-glycerol-based OECT achieves a high transconductance of 10.1 mS. At 50% tensile strain, the ECG signal acquisition of CSglycerol-based OECT showed significant attenuation (Fig. 4b). According to the optical microscope images, severe microcrack extension was observed for CS-glycerol layer (Fig. S6), while the channel layer remained intact under strain (Fig. S7). This suggests that the limited ductility of CS-glycerol electrolyte leads to failure of the electrolyte-semiconductor interface [53]. In contrast, CS-PHEA-based OECT maintains a stable recording of ECG analog signals under 50% strain and shows a high SNR above 30 dB (Fig. 4c, d), demonstrating a promising potential for operando measurement of epidermal electrophysiology signals.

CONCLUSIONS

In summary, we have successfully manufactured stretchable

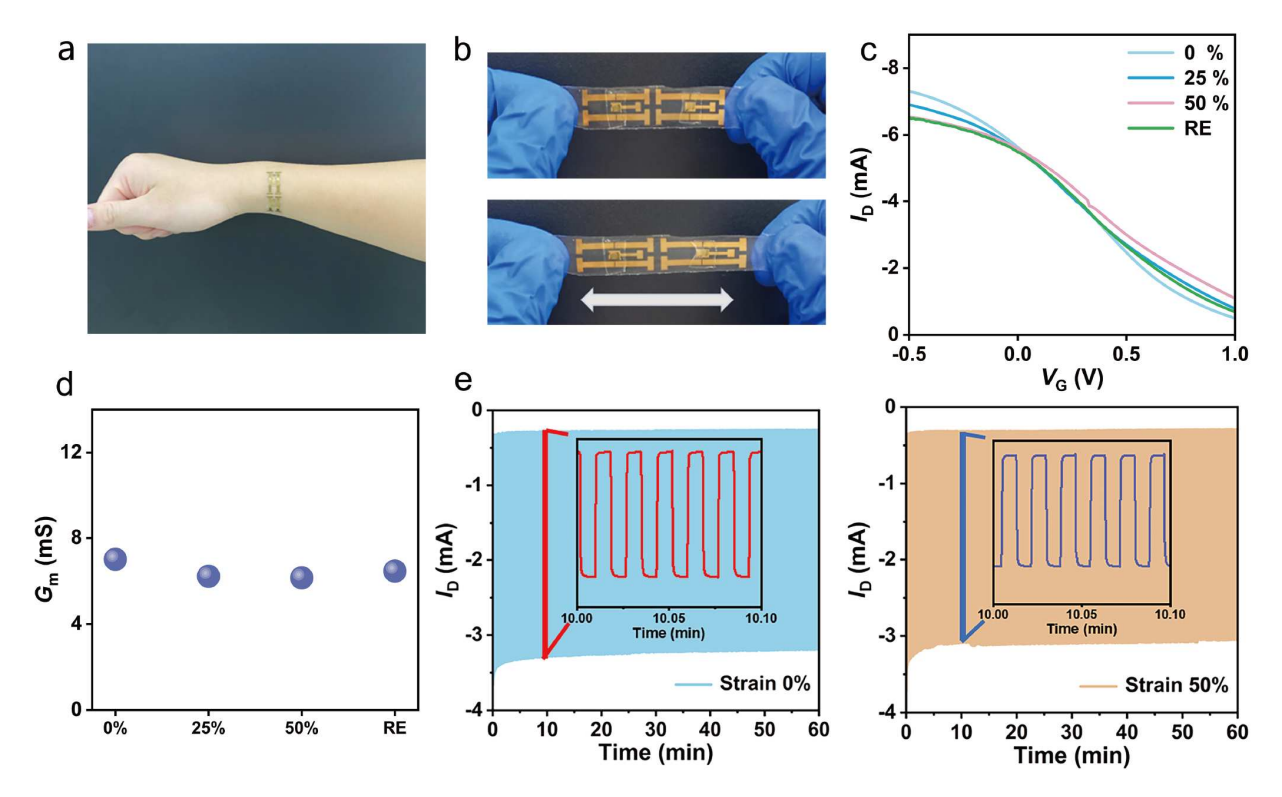


Figure 3 Stretchable solid-state OECT. (a) Photograph of stretchable solid-state OECT. (b) Illustrations of the intrinsically stretchable solid-state OECT. (c) Transfer plots of OECTs under various strains (0% to 50%) applied parallel (ε/l) to the channel length (L=200 μm, W=1800 μm). (d) $G_{\rm m}$ of the intrinsically stretchable OECT under various strains (0% to 50%). (e) Transient characteristics of stretchable solid-state OECT (under strain 0% and 50%) with alternating gate potentials ($V_{\rm G}$ =0.8 and 0 V, and $V_{\rm D}$ =-0.5 V) for 60 min.

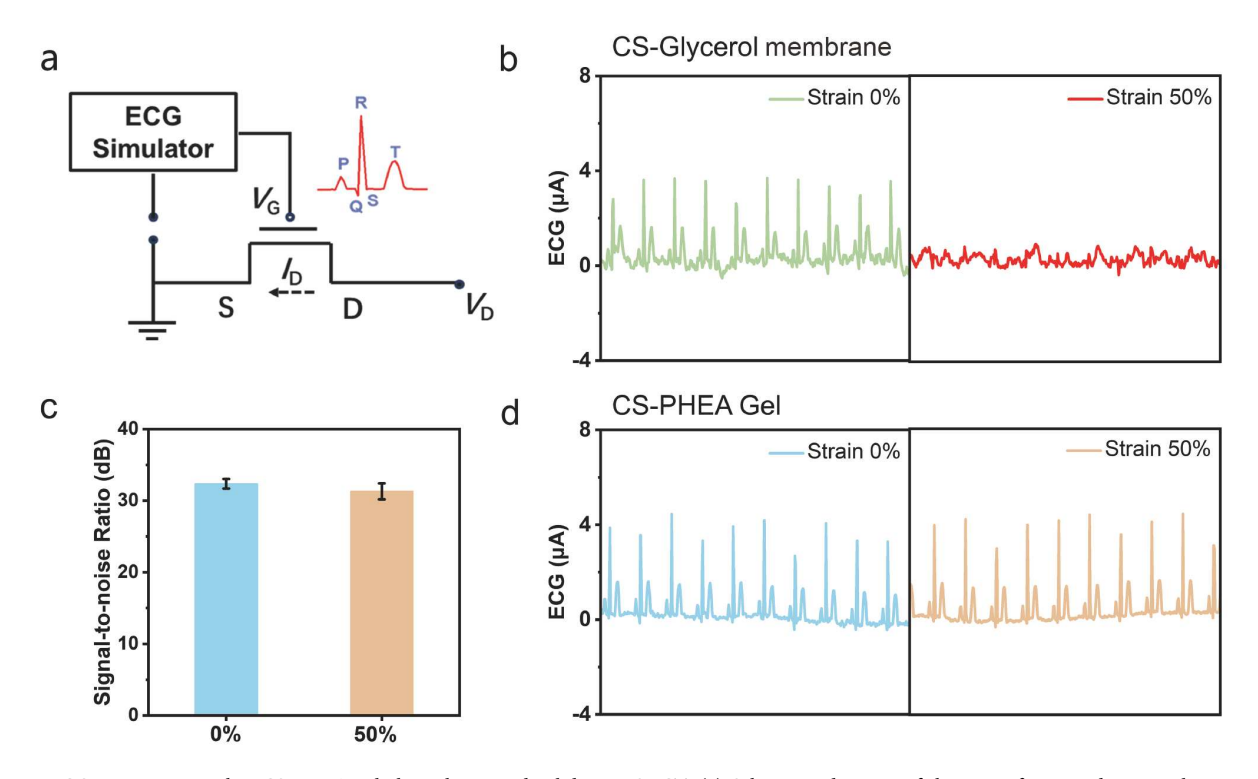


Figure 4 ECG acquisition with a CS-PHEA gel electrolyte-gated solid-state OECT. (a) Schematic diagram of the setup for recording simulator-generated ECG waveforms and spectra using CS-PHEA gel electrolyte-gated solid-state OECT. (b) Solid-state OECT based on CS ion membrane is used to record ECG signal under 50% strain. (c) SNR of CS-PHEA gel electrolyte-gated solid-state OECT output signals under different stretching conditions (statistics are conducted based on five consecutive peak data). (d) Recording simulator-generated ECG waveforms and spectra using a stretchable CS-PHEA gel electrolyte-gated solid-state OECT under different strains (0% to 50%).

solid-state OECT by developing a soft (Young's modulus of 114 kPa) and stretchable (elongation break at 640%) CS-PHEA gel electrolyte and integrating it with a stretchable PEDOT:PSS layer while maintaining the mechanical and electrical properties of both components. The OECT device has excellent amplification performance ($[\mu C^*]$ =317.71 ± 11.61 F cm⁻¹ V⁻¹ s⁻¹), and we successfully prepared high-uniformity arrays with the average transconductance of 7.89 mS. The good mechanical adaptation of the gel electrolyte facilities the achievement stable electrophysiological signal acquisition under 50% strain with a high-quality SNR output (~30 dB). This work provides a simple, low-cost, and efficient material design for gel electrolytes, and represents an important step in the fabrication of stretchable solid-state OECTs. It promises long-term development for high-resolution integrated biointerfaces based on organic electronics.

Received 2 April 2025; accepted 21 May 2025; published online 31 July 2025

- 1 Pitsalidis C, Pappa AM, Boys AJ, et al. Organic bioelectronics for in vitro systems. Chem Rev, 2022, 122: 4700–4790
- 2 Tsarfati Y, Bustillo KC, Savitzky BH, et al. The hierarchical structure of organic mixed ionic-electronic conductors and its evolution in water. Nat Mater, 2025, 24: 101–108
- 3 Rivnay J, Owens RM, Malliaras GG. The rise of organic bioelectronics. Chem Mater, 2013, 26: 679–685
- 4 Chen Y, Li S, Shen Z, et al. In-situ temperature-controllable grazing incidence X-ray scattering of semiconducting polymer thin films under stretching. Sci China Mater, 2024, 67: 3917–3924
- 5 Liao C, Zhang M, Yao MY, et al. Flexible organic electronics in biology: materials and devices. Adv Mater, 2015, 27: 7493–7527
- 6 Torricelli F, Adrahtas DZ, Bao Z, et al. Electrolyte-gated transistors for enhanced performance bioelectronics. Nat Rev Methods Primers, 2021, 1: 65
- 7 Dai Y, Dai S, Li N, et al. Stretchable redox-active semiconducting polymers for high-performance organic electrochemical transistors. Adv Mater, 2022, 34: e2201178
- 8 Someya T, Bao Z, Malliaras GG. The rise of plastic bioelectronics. Nature, 2016, 540: 379–385
- 9 Liu R, Zhu X, Duan J, et al. Versatile neuromorphic modulation and biosensing based on n-type small-molecule organic mixed ionic-electronic conductors. Angew Chem Int Ed, 2023, 63: e202315537
- 10 Rivnay J, Inal S, Salleo A, et al. Organic electrochemical transistors. Nat Rev Mater, 2018, 3: 17086
- Marks A, Griggs S, Gasparini N, et al. Organic electrochemical transistors: an emerging technology for biosensing. Adv Mater Inter, 2022, 9: 2102039
- 12 Zhang C, Zheng Y, Li Y, et al. Polythiophenes for high-performance ntype organic electrochemical transistors. Adv Funct Mater, 2025, 35: 2419706
- 13 Lu D, Chen H. Solid-state organic electrochemical transistors (OECTs) based on gel electrolytes for biosensors and bioelectronics. J Mater Chem A, 2025, 13: 136–157
- 14 Li S, Gao M, Zhou K, et al. Achieving record-high stretchability and mechanical stability in organic photovoltaic blends with a diluteabsorber strategy. Adv Mater, 2024, 36: 2307278
- 15 Chen Y, Chen L, Geng B, et al. Triple-network-based conductive polymer hydrogel for soft and elastic bioelectronic interfaces. Smart-Mat, 2023, 5: e1229
- 16 Yao Y, Huang W, Chen J, et al. Flexible and stretchable organic electrochemical transistors for physiological sensing devices. Adv Mater, 2023, 35: e2209906
- 17 Li Y, Zhao Y, Yang R, et al. Flexible electrodes with enhancement of electronic-ionic conductivity for electrophysiological signal monitoring. Wearable Electron, 2024, 1: 228–235
- 18 An C, Dong W, Yu R, et al. High-performance n-type stretchable

- semiconductor blends for organic thin-film transistors and artificial synapses. Chem Mater, 2023, 36: 450–460
- Huang L, Zhao D, Yan X, et al. Organic electrochemical transistors: from lithography to large-scale printing. Adv Elect Mater, 2025, 11: 2400474
- 20 Chen S, Surendran A, Wu X, et al. Contact modulated ionic transfer doping in all-solid-state organic electrochemical transistor for ultrahigh sensitive tactile perception at low operating voltage. Adv Funct Mater, 2020, 30: 2006186
- 21 Jo YJ, Kwon KY, Khan ZU, et al. Gelatin hydrogel-based organic electrochemical transistors and their integrated logic circuits. ACS Appl Mater Interfaces, 2018, 10: 39083–39090
- Yu Y, Zhu G, Lan L, et al. N-type glycolated imide-fused polycyclic aromatic hydrocarbons with high capacity for liquid/solid-electrolytebased electrochemical devices. Adv Funct Mater, 2023, 33: 2300012
- 23 Liu X, Liu J, Lin S, et al. Hydrogel machines. Mater Today, 2020, 36: 102–124
- 24 Wang Y, Wustoni S, Surgailis J, et al. Designing organic mixed conductors for electrochemical transistor applications. Nat Rev Mater, 2024, 9: 249–265
- 25 Chen Z, Ding X, Wang J, et al. π-conjugated polymers for high-performance organic electrochemical transistors: molecular design strategies, applications and perspectives. Angew Chem Int Ed, 2025, 64: e202423013
- 26 Lei Y, Li P, Zheng Y, et al. Materials design and applications of n-type and ambipolar organic electrochemical transistors. Mater Chem Front, 2024, 8: 133–158
- 27 Zhao Z, Fan X, Wang S, et al. Natural polymers-enhanced doublenetwork hydrogel as wearable flexible sensor with high mechanical strength and strain sensitivity. Chinese Chem Lett, 2023, 34: 107892
- 28 Lee H, Lee S, Lee W, et al. Ultrathin organic electrochemical transistor with nonvolatile and thin gel electrolyte for long-term electrophysiological monitoring. Adv Funct Mater, 2019, 29: 1906982
- 29 Wang J, Lee S, Yokota T, et al. Gas-permeable organic electrochemical transistor embedded with a porous solid-state polymer electrolyte as an on-skin active electrode for electrophysiological signal acquisition. Adv Funct Mater, 2022, 32: 2200458
- 30 Su X, Wu X, Chen S, et al. A highly conducting polymer for self-healable, printable, and stretchable organic electrochemical transistor arrays and near hysteresis-free soft tactile sensors. Adv Mater, 2022, 34: e2200682
- 31 Tang H, Liang Y, Yang CY, et al. Polyethylene glycol-decorated n-type conducting polymers with improved ion accessibility for high-performance organic electrochemical transistors. Mater Horiz, 2024, 11: 5419–5428
- 32 Welch ME, Doublet T, Bernard C, et al. A glucose sensor via stable immobilization of the GOx enzyme on an organic transistor using a polymer brush. J Polym Sci Part A-Polym Chem, 2014, 53: 372–377
- 33 Zhu Z, Pang Y, Li Y, et al. The rising of flexible organic electrochemical transistors in sensors and intelligent circuits. ACS Nano, 2025, 19: 4084–4120
- 34 Zheng X, Hu M, Liu Y, et al. High-resolution flexible electronic devices by electrohydrodynamic jet printing: from materials toward applications. Sci China Mater, 2022, 65: 2089–2109
- 35 Yu D, Li X, Xu J. Safety regulation of gel electrolytes in electrochemical energy storage devices. Sci China Mater, 2019, 62: 1556–1573
- 36 Jiang Y, Zhang Z, Wang YX, et al. Topological supramolecular network enabled high-conductivity, stretchable organic bioelectronics. Science, 2022, 375: 1411–1417
- 37 Bai Y, Li W, Tie Y, et al. A stretchable polymer conductor through the mutual plasticization effect. Adv Mater, 2023, 35: e2303245
- 38 Torğut G, Yazdıç FC, Gürler N. Synthesis, characterization, pH-sensitive swelling and antimicrobial activities of chitosan-graft-poly(hydroxyethyl methacrylate) hydrogel composites for biomedical applications. Polym Eng Sci, 2022, 62: 2552–2559
- 39 Cea C, Spyropoulos GD, Jastrzebska-Perfect P, et al. Enhancement-mode ion-based transistor as a comprehensive interface and real-time processing unit for in vivo electrophysiology. Nat Mater, 2020, 19: 679–686

- 40 Than-ardna B, Tamura H, Furuike T. Preparation, characterization, and properties of chitosan-based semi-interpenetrating polymer networks and poly(2-hydroxyethyl methacrylate) structure. Macro Chem Phys, 2022, 223: 2200282
- 41 Yao P, Bao Q, Yao Y, *et al.* Environmentally stable, robust, adhesive, and conductive supramolecular deep eutectic gels as ultrasensitive flexible temperature sensor. Adv Mater, 2023, 35: 2300114
- 42 Ohm Y, Pan C, Ford MJ, et al. An electrically conductive silver–polyacrylamide–alginate hydrogel composite for soft electronics. Nat Electron, 2021, 4: 185–192
- 43 Guo B, Yao M, Chen S, et al. Environment-tolerant conductive eutectogels for multifunctional sensing. Adv Funct Mater, 2024, 34: 2315656
- 44 Lee Y, Oh JY, Xu W, et al. Stretchable organic optoelectronic sensorimotor synapse. Sci Adv, 2018, 4: eaat7387
- 45 Yu C, Shi M, He S, et al. Chronological adhesive cardiac patch for synchronous mechanophysiological monitoring and electrocoupling therapy. Nat Commun, 2023, 14: 6226
- 46 Oh JY, Rondeau-Gagné S, Chiu YC, et al. Intrinsically stretchable and healable semiconducting polymer for organic transistors. Nature, 2016, 539: 411–415
- 47 Cea C, Zhao Z, Wisniewski DJ, et al. Integrated internal ion-gated organic electrochemical transistors for stand-alone conformable bioelectronics. Nat Mater, 2023, 22: 1227–1235
- 48 Dai Y, Hu H, Wang M, et al. Stretchable transistors and functional circuits for human-integrated electronics. Nat Electron, 2021, 4: 17–29
- 49 Yang A, Song J, Liu H, et al. Wearable organic electrochemical transistor array for skin-surface electrocardiogram mapping above a human heart. Adv Funct Mater, 2023, 33: 2215037
- 50 Chen J, Huang W, Zheng D, et al. Highly stretchable organic electrochemical transistors with strain-resistant performance. Nat Mater, 2022, 21: 564–571
- 51 Zhang S, Hubis E, Tomasello G, *et al.* Patterning of stretchable organic electrochemical transistors. Chem Mater, 2017, 29: 3126–3132
- 52 Zhong Y, Lopez-Larrea N, Alvarez-Tirado M, et al. Eutectogels as a semisolid electrolyte for organic electrochemical transistors. Chem Mater, 2024, 36: 1841–1854
- 53 Khodagholy D, Rivnay J, Sessolo M, et al. High transconductance organic electrochemical transistors. Nat Commun, 2013, 4: 2133

Acknowledgement This work was supported by the National Key Research and Development Program of China (2022YFF1202902 and 2023YFB3609000), the National Natural Science Foundation of China (52273192 and 52121002), and the Haihe Laboratory of Sustainable Chemical Transformations.

Author contributions Wang YX and Hu W conceived the idea and directed the project; Wang YX and Tang L designed and engineered the samples; Tang L carried out most of the experiments; Zheng X and Sun M performed some measurements; Tang L wrote the paper with support from Wang YX and Hu W. Ren X, Huang W and Guo C provided experimental guidance. All authors contributed to the general discussion.

Conflict of interest The authors declare that they have no conflict of interest.

Supplementary information Supplementary materials are available in the online version of the paper.



Liqun Tang is a PhD student under the supervision of Prof. Wenping Hu and Yi-Xuan Wang at the Department of Chemistry, School of Science, Tianjin University, and the Collaborative Innovation Center of Chemical Science and Engineering (Tianjin). His research interests are organic optoelectronic materials and flexible electronic devices.



Yi-Xuan Wang is a professor at Tianjin University. He received his BSc (2010) and PhD (2015) degrees from Nankai University. His research focuses on the development of stretchable conducting/semiconducting polymers by supramolecular chemistry.



Wenping Hu is a professor at Tianjin University. He received his PhD degree from Institute of Chemistry, Chinese Academy of Sciences (ICCAS). Then he joined Osaka University and Stuttgart University as a research fellow of Japan Society for the Promotion of Sciences and an Alexander von Humboldt fellow, respectively. Then he joined ICCAS as a full professor. He moved to Tianjin University in 2013. His research focuses on organic optoelectronics.

光图案化凝胶电解质实现高性能可拉伸固态有机电 化学晶体管

汤立群 1 , 郑雪 1 , 孙明源 1 , 任晓辰 1,2,3 , 黄伟 4 , 叶龙 1,5 , 郭传飞 6 , 王以轩 1,2,3* , 胡文平 1,2,3*

摘要 有机电化学晶体管(OECT)作为转导放大器,在生物电子集成和可穿戴技术方面显示出巨大潜力.然而,传统OECT柔性欠佳,且依赖液态电解质作栅控介质,在生物表面共形传感的稳定性方面存在局限.我们发展了一种基于双网络聚合物结构的可拉伸凝胶电解质,它同时具备了优异的机械顺应性和高离子电导率.借由光交联基团,该凝胶电解质可方便地实现光图案化,基于其栅控的OECT阵列表现出均一的电学性能.此外,这类固态OECT在50%应变下可稳定运行,并成功实现了机械形变状态下的持续心电图监测,验证了其在需要长期生物传感的动态医疗系统中的应用潜力.